very small d [see, e.g., Eq. (23)] while for d larger than several nm Γ_{jk}^{nr} is dominated by the $l = 1$ term. In fact, in a wide range d, nonradiative coupling between dipoles is mainly through the optically active *dipole* plasmon mode that does not cause mixing between superradiant and subradiant states. Namely, it can be easily seen from Eq. (23) that the eigenstates of the $l = 1$ term in Γ_{jk}^{nr} are the same as those of Γ_{jk}^{r} so the corresponding eigenvalues are similarly given by $\Gamma_{\mu}^{nr} = (N\Gamma^{nr}/3)\,\lambda_{\mu}$. Thus, the superradiant quantum efficiency

$$Q_{\mu} = \frac{\Gamma_{\mu}^{r}}{\Gamma_{\mu} + \Gamma_{0}^{nr}} = \frac{\Gamma^{r}}{\Gamma + 3\Gamma_{0}^{nr}/N\lambda_{\mu}} \tag{41}$$

only weakly depends on N. Therefore, the sum in Eq. (37) includes just three terms, yielding

$$W_{ens} = \frac{\hbar kc}{2}\,Q_{ens} = \frac{\hbar kc}{2}\sum_{\mu=1}^{3}\frac{\Gamma^{r}}{\Gamma + 3\Gamma_{0}^{nr}/N\lambda_{\mu}}. \tag{42}$$

For high-yield (small Γ_{0}^{nr}) emitters, we obtain Eq. (1) and hence $W_{ens} \approx 3W$. In contrast, the radiated *power*,

$$P_{ens} = \frac{\hbar kc}{2}\sum_{\mu=1}^{3} Q_{\mu}\Gamma_{\mu}^{r} \simeq N\left(\frac{\hbar kc}{2}\,Q\Gamma^{r}\right) = NP, \tag{43}$$

scales with the ensemble size due to shorter (by factor $N/3$) radiative lifetime of superradiant states.

For low-yield emitters (large Γ_{0}^{nr}), the relation Eq. (1) holds only approximately. However, it is evident from comparison of Eqs. (36) and (42) that here the relative effect of internal relaxation is much weaker than for usual cooperative emission. Numerical results for both high-yield and low-yield emitters are presented below.

Let us now turn to the role of interactions between dipoles in the ensemble, which is the main subject of this paper. Interactions play critical role in cooperative emission since they introduce a disorder into system energy spectrum by causing random shifts of individual dipole frequencies.[24–26] In the conventional cooperative emission, the main disorder effect is to split the narrow subradiant peak in the ensemble emission spectra.[25] In the presence of metal nanostructure, radiation of subradiant states is expected to be quenched by much faster nonradiative losses in the metal. The crucial question is, however, whether interactions between closely spaced individual dipoles can significantly alter the structure of collective eigenstates. In the remaining part of the paper, we present the results of our numerical simulations of cooperative emission fully incorporating both direct and plasmon-mediated interactions.

We consider an ensemble of N molecular dyes attached to an Ag spherical particle with radius $R = 20$ nm via molecular linkers with approximately same length. The system is embedded in aqueous solution with dielectric constant $\epsilon_0 = 1.77$, and two types of dyes with quantum efficiencies $q = 0.3$ and $q = 0.95$ are used in the calculations. A distinguishing feature of this system is a strong

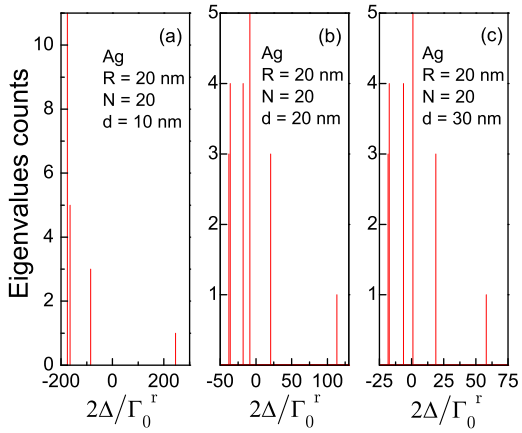

FIG. 2: (Color online) Distribution of energy shifts for 20 dipoles in C20 configuration around Ag NP at several distances to its surface.

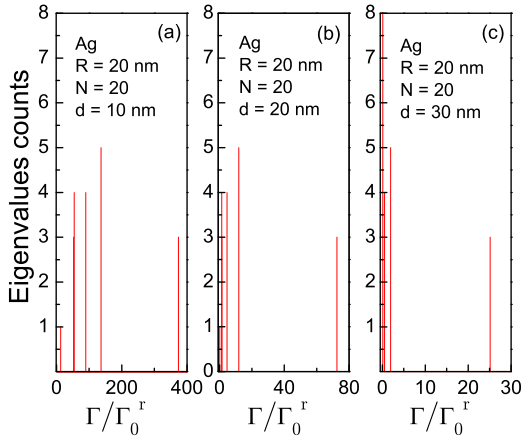

FIG. 3: (Color online) Distribution of decay rates for 20 dipoles in C20 configuration around Ag NP at several distances to its surface.

effect of interactions on its geometry.[16] The flexible linker molecules hold the attached dyes with certain orientation of their dipole moments, so that repulsive inter-molecule interactions compel the dyes to form a spatially ordered structure on spherical surface. In our simulations, the dyes with normal dipole orientations were located at the sites of spherical lattice, specifically, fullerenes C20, C32, C60, and C80, and, in some calculations, we included random deviations from the ideal lattice positions. The system eigenstates are found by numerical diagonalization of self-energy matrix, $\Sigma_{jk} = \Delta_{jk} - \frac{i}{2}\Gamma_{jk}$, with its real and imaginary parts given by Eqs. (24) and (23), respectively. Calculations were carried at the SP energy of 3.0 eV, the size-dependent Landau damping was incorporated for all plasmon modes, and NP polarizabilities, Eq. (13), with angular momenta up to $l = 30$, were calculated using the experimental bulk Ag complex dielectric function.

Figures 2 and 3 show distribution of real and imag-